Int J Ophthalmol, Vol. 10, No. 8, Aug.18, 2017 www.ijo.cn
Tel:8629-82245172 8629-82210956 Email:ijopress@163.com

• Clinical Research •

Area and volume ratios for prediction of visual outcome in idiopathic macular hole

Xing-Yun Geng[1,2], Hui-Qun Wu[2], Jie-Hui Jiang[1], Kui Jiang[2], Jun Zhu[3], Yi Xu[3], Jian-Cheng Dong[2], Zhuang-Zhi Yan[1]

[1]The Institute of Biomedical Engineering, School of Communication and Information Engineering, Shanghai University, Shanghai 200444, China
[2]Department of Medical Informatics, Medical School of Nantong University, Nantong 226001, Jiangsu Province, China
[3]Department of Ophthalmology, Affiliated Hospital of Nantong University, Nantong 226001, Jiangsu Province, China
Correspondence to: Zhuang-Zhi Yan. The Institute of Biomedical Engineering, School of Communication and Information Engineering, Shanghai University, Shanghai 200444, China. zzyan@shu.edu.cn; Jian-Cheng Dong. Department of Medical Informatics, Medical School of Nantong University, Nantong 226001, Jiangsu Province, China. dongjc@ntu.edu.cn
Received: 2016-11-07 Accepted: 2017-04-26

Abstract

● AIM: To predict the visual outcome in patients undergoing macular hole surgery by two novel three-dimensional morphological parameters on optical coherence tomography (OCT): area ratio factor (ARF) and volume ratio factor (VRF).

● METHODS: A clinical case series was conducted, including 54 eyes of 54 patients with an idiopathic macular hole (IMH). Each patient had an OCT examination before and after surgery. Morphological parameters of the macular hole, such as minimum diameter, base diameter, and height were measured. Then, the macular hole index (MHI), tractional hole index (THI), and hole form factor (HFF) were calculated. Meanwhile, novel postoperative macular hole (MH) factors, ARF and VRF were calculated by three-dimensional morphology. Bivariate correlations were performed to acquire asymptotic significance values between the steady best corrected visual acuity (BCVA) after surgery and 2D/3D arguments of MH by the Pearson method with two-tailed test. All significant factors were analyzed by the receiver operating characteristic (ROC) curve analysis of SPSS software which were responsible for vision recovery. ROC curves analyses were performed to further discuss the different parameters on the prediction of visual outcome.

● RESULTS: The mean and standard deviation values of patients' age, symptoms duration, and follow-up time were 64.8±8.9y (range: 28-81), 18.6±11.5d (range: 2-60), and 11.4±0.4mo (range: 6-24), respectively. Steady-post-BCVA analyzed with bivariate correlations was found to be significantly correlated with base diameter (r=0.521, P<0.001), minimum diameter (r=0.514, P<0.001), MHI (r=-0.531, P<0.001), THI (r=-0.386, P=0.004), HFF (r=-0.508, P<0.001), and ARF (r=-0.532, P<0.001). Other characteristic parameters such as age, duration of surgery, height, diameter hole index, and VRF were not statistically significant with steady-post-BCVA. According to area under the curve (AUC) values, values of ARF, MHI, HFF, minimum diameter, THI, and base diameter are 0.806, 0.772, 0.750, 0.705, 0.690, and 0.686, respectively. However, Steady-post-BCVA analysis with bivariate correlations for VRF was no statistical significance. Results of ROC curve analysis indicated that the MHI value, HFF, and ARF was greater than 0.427, 1.027 and 1.558 respectively which could correlate with better visual acuity.

● CONCLUSION: Compared with MHI and HFF, ARF could effectively express three-dimensional characteristics of macular hole and achieve better sensitivity and specificity. Thus, ARF could be the most effective parameter to predict the visual outcome in macular hole surgery.

● KEYWORDS: optical coherent imaging; prognostic evaluation; idiopathic macular hole; morphological features
DOI:10.18240/ijo.2017.08.12

Citation: Geng XY, Wu HQ, Jiang JH, Jiang K, Zhu J, Xu Y, Dong JC, Yan ZZ. Area and volume ratios for prediction of visual outcome in idiopathic macular hole. *Int J Ophthalmol* 2017;10(8):1255-1260

INTRODUCTION

Idiopathic macular hole (IMH) without fundus-related disease occurs in the macular zone of normal eyes, generally in individuals aged over 50y. The female to male ratio is approximately 2:1[1]. Affected patients suffer from severe visual impairment.

Vitreous surgery within the joint boundary membrance peeling and injection of inert gas is the main method for clinic treatment of IMH[2]. Extensive research has been explored to study the prognostic factors after surgery[3-6]. Clinical doctors using spectral-domain optical coherence tomography (SD-OCT) can effectively observe the structural changes in the morphology of IMH in both preoperative and postoperative patients. A lot of literature has been studied about the optical coherence tomography (OCT) image of quantitative parameters to predict IMH postoperative vision in advance, such as macular hole index (MHI), tractional hole index (THI), and hole form factor (HFF)[7-8].

In order to show the complete 3D morphology of the macular hole, OCT scanning equipment manufacturers including Zeiss[9], Topcon[10], and Heidelberg[11] constantly developed new 3D OCT hardware and software. Accordingly, there was a lot of related research based on 3D OCT. Scheibe *et al*[12] reconstructed 3D foveal surface from OCT data to observe the whole range of asymmetric. Haas *et al*[13] analyzed choroidal thickness with 3D-OCT. Brionesr *et al*[14] reported a spectral OCT system with the internal 3D microstructure and displacement maps from a poly-methyl-methacrylate sample. Todorich *et al*[15] evaluated the impact of swept-source microscope-integrated optical coherence tomography (MI-OCT) and tissue-level 3D imaging on ophthalmology residents' performance of ophthalmic microsurgical maneuvers. Hu *et al*[16] developed a 3D graph-based approach to identify the 3D choroidal layer in SD-OCT images by using the Bruch's membrane opening prior knowledge information. Three-dimensional display is steadily becoming the focus of research and development.

Macular hole (MH) is a common age-related eye disease[17-18], and IMH is one of the most common types of MH[19]. IMH often causes macular degeneration, swelling, and rupture in patients. As most human vision comes from the macular center, MH could cause marked decline in vision. Vitrectomy is a common clinical surgical method[20] widely used in the treatment of MH. Post-operative visual acuity of MH surgery is diverse with different classifications and form of MH morphology. Therefore, designing effective factors to predict postoperative visual recovery became very important.

To explore effective factors, several research groups proposed various morphological characteristics such as MHI, HFF, THI, diameter hole index (DHI), minimum diameter (MD), and base diameter (BD)[7-8]. However, these parameters only expressed quantitative information of a certain direction slice and could not effectively express the direction of different opposites. New clinical parameters are required.

All proposed MH parameters, which cannot effectively express 3D characteristics of MH, are measured on a single slice image of OCT. Therefore, novel MH's factors that contain area ratio factor (ARF) and volume ratio factor (VRF) were designed and generated by 3D morphology to predict post-operative patients' vision outcome with IMH.

SUBJECTS AND METHODS

Patients This was a retrospective clinical case series of 54 eyes (19 left eyes and 35 right eyes) from 54 patients (15 male and 39 female). Patients were diagnosed as having IMHs and proceeded to have vitreous surgery. Cases were collected from January 2013 until March 2015 in Affiliated Hospital of Nantong University Eye Center. The MH stages in patients' eyes were II (24 eyes), III (10 eyes), and IV (20 eyes) according to the GASS standard. The lens statuses of pre-operative patients' eyes were opacity (9 eyes) and lucency (45 eyes). The lens statuses of post-operative patients' eyes were intraocular lens (9 eyes) and original lens (45 eyes). The mean and standard deviation values of age, symptoms duration, and follow-up time were 64.8±8.9y (range: 28-81), 18.6±11.5d (range: 2-60), and 11.4±0.4mo (range: 6-24), respectively. The inclusion criterion was diagnosis of idiopathic full-thickness macular holes on slit-lamp microscopy and ophthalmoscopy and OCT examination. Patients with other eye diseases that may affect vision, including high myopia, glaucoma, optic neuropathy, proliferative vitreous retinopathy, retinal detachment, and fundus of other diseases were excluded. Patient selection process was approved by the hospital's ethics committee and the study followed the tenets of the Declaration of Helsinki.

Surgical Methods A three-port pars plana 23-gauge vitrectomy was performed on all patients by the same surgeon. The main process includes: 1) making core vitrectomy and triamcinolone acetonide assisted (10 mg/mL) posterior vitreous detachment; 2) injecting of indocyanine green (ICG, 5 mg/mL) on the surface of anterior limiting membrane; 3) using the flute needle gettering ICG after about 60s; 4) peeling 3 to 4 disc diameter centering of inner limiting membrane (ILM) around the macula; 5) filling with 14% C3F8 into the vitreous cavity. Patients were in the face-down position after surgery for one week until C3F8 gas was completely absorbed. Patients with lens opacity had undergone concurrent cataract surgery.

Measure Parameters All patients' OCT images were recorded before, after, and follow-up OCT examination images. The whole OCT images were acquired by Carl Zeiss CIRRUS HD-OCT 4000. The machine has scanned macular with 6 mm width, 6 mm height and 2 mm depth. The horizontal and vertical number of slices is 512 and 128, respectively. Each slice image size is 300×200 in pixel. In the tissue, the resolution is 5 μm in axial and 15 μm in lateral.

The 2D parameters are shown in Figure 1. BD, MD, height (H), left arm length (LA), and right arm length (RA) in Figure 1B were manually measured by the software measuring tool on the OCT machine. All 2D parameters were measured thrice for each eye and assigned as the average value by two clinicians. When there was a disagreement between them, it was verified by a third doctor in order to ensure the accuracy of measurement. The MHI was defined by Kusuhara *et al*[8]. The THI and DHI was defined by Ruiz-Moreno *et al*[1]. The HFF was defined by Ullrich *et al*[7]. The values were calculated using the following formulae:

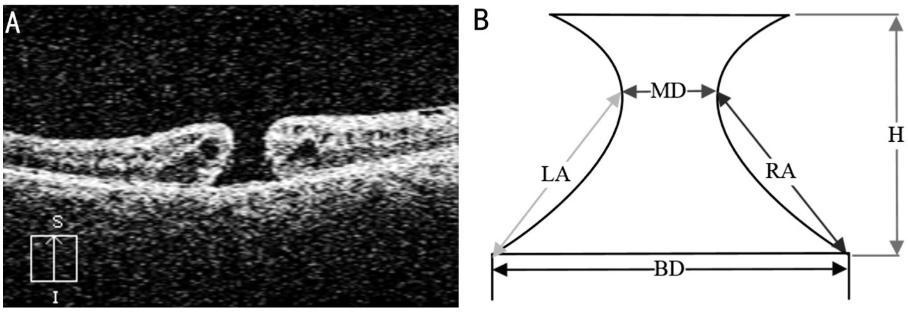

Figure 1 The two-dimensional parameters A: A real OCT image slices; B: The corresponding measurement simplified diagram.

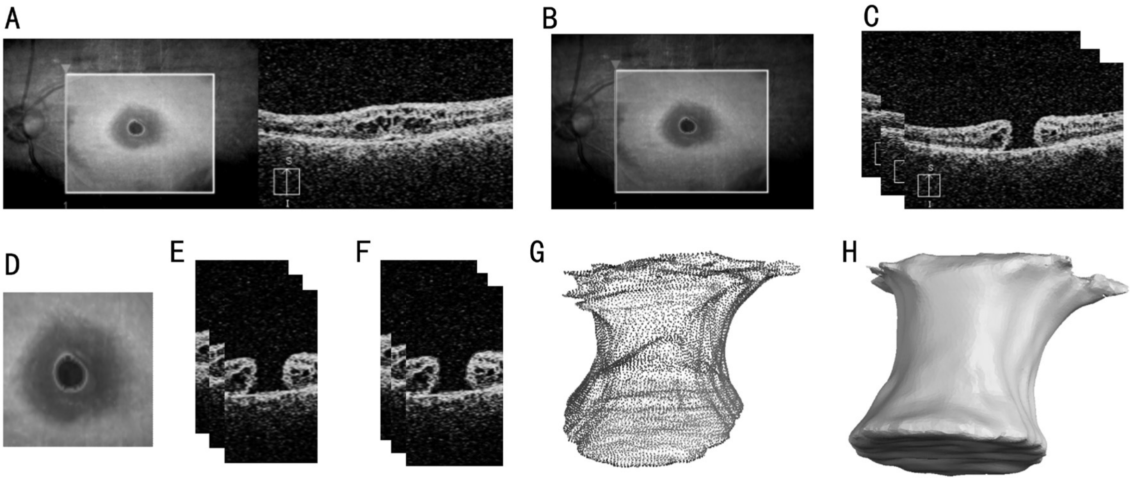

Figure 2 Reconstruction experiment screenshots A: OCT image; B: Fundus image; C: Slice images; D: Zone of MH on the fundus image; E: Zone of MH on the slice image; F: boundary of the MH (red); G: 3D points picture of MH; H: Reconstruction of 3D structure of MH.

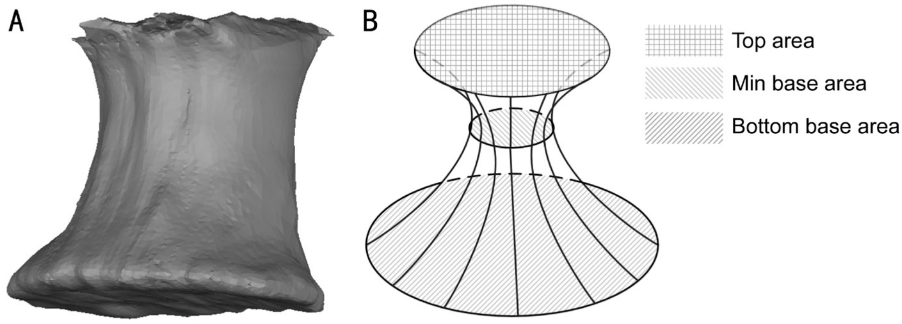

Figure 3 The three-dimensional parameters A: A real MH 3D reconstruction image; B: Measuring the corresponding area and volume.

MHI=H/BD F1

THI=MD/BD F2

DHI=H/MD F3

HFF=(LA+RA)/BD F4

The reconstructed 3D model of MH was formed of the following steps. 1) The OCT file was read from the hard disk. 2) The fundus and slice images were obtained. 3) MH position on fundus image was obtained to confirm the MH region on slices. 4) Each boundary point of MH was manually drawn by clinicians. 5) The points were translated to 3D coordinates according to scanning interval of the OCT machine. 6) These 3D points were imported into Meshlab software v1.3.3 (64-bit version) to reconstruct 3D MH. 7) Particular zone's area and volume were measured using the measurement tools. The reconstruction experiment screenshots are shown in Figure 2.

Considering that MH is a 3D structure, two novel 3D factors for the 3D structure of MH were defined by our research group: ARF and VRF. Inferior volume contains the region between the minimum and bottom base. The related parameters are shown in the Figure 3.

ARF=Body surface area/bottom base area F5

VRF=Inferior volume/all volume F6

Statistical Analysis Parameters including pre-best corrected visual acuity (BCVA), post-operational follow-up BCVA, BD, MD, H, MHI, THI, HFF, ARF, and VRF were analyzed. Steady-post-BCVA stands for patients' vision unchanged at least 6mo in last two visits after surgery. Pre-BCVA and steady-post-BCVA were recorded in decimal visual acuity and converted to logMAR equivalent for statistical analyses[21].

First, pre-BCVA was analyzed for its correlation with steady post-operational follow-up BCVA (steady-post-BCVA) by

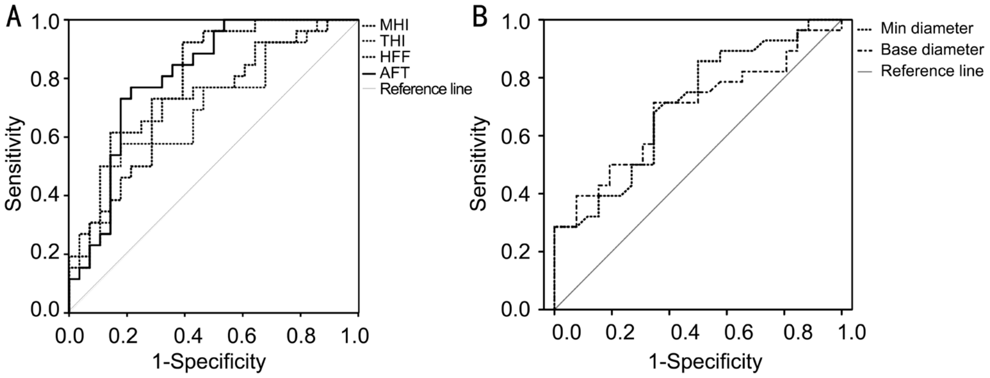

Figure 4 ROC curves A: Positive correlation parameters; B: Negative correlation parameters.

nonparametric tests through Wilcoxon-rank sum methods. Then, bivariate correlations were performed to acquire asymptotic significance values between the steady BCVA after surgery and 2D/3D arguments of MH by the Pearson method with two-tailed test. Finally, receiver operating characteristic (ROC) curves were used to quantify the performance of MD, BD, MHI, THI, and ARF for better visual outcome after surgery, by means of sensitivity, specificity, area under the curve (AUC), and corresponding 95% confidence intervals (CIs). Only AUC>0.5 indicates effective diagnostic value. If 0.5<AUC≤0.7, it indicates low accuracy. If 0.7<AUC≤0.9, it indicates moderate accuracy. If AUC>0.9, it indicates higher accuracy. If AUC=0.5, it indicates that the diagnostic method does not work completely and thereby has no diagnostic value. We investigated the optimum cut-off value for diagnosis by maximizing the sum of sensitivity and specificity and minimizing the distance of the cut-off value to the top-left corner of the ROC curve. P<0.05 (two-sided test) was considered significant. All statistical analyses were performed with SPSS 18.0 software (SPSS, IBM Software Company).

RESULTS

The mean and standard deviation values of MD, BD, height, logMAR pre-BCVA and logMAR steady-post-BCVA were 446.5±168.3 μm (range: 99-857), 888.6±300.4 μm (range: 212-1516), 666.9±138.7 μm (range: 281-1031), 0.80±0.23 (range: 0.4-1.0) and 0.41±0.24 (range: 0.1-1.0), respectively. The whole BCVA of 54 cases was effectively elected after surgery. To evaluate surgery results by BCVA, we defined three BCVA statuses: if the patient's pro-BCVA improved more than two lines in visual acuity chart, it means improvement of BCVA; if the patient's pro-BCVA fluctuates in one lines in visual acuity chart, it means unchanged of BCVA; if the patient's pro-BCVA declined more than two lines in visual acuity chart, it means worsened of BCVA. The results showed that BCVA of 40 (74.1%) eyes showed improvement, 11 (20.4%) remained unchanged, 3 (5.5%) worsened. Steady-post-BCVA had asymptotic significations with pre-BCVA in Wilcoxon signed rank test (P<0.01).

Table 1 The *r* and *P* value of bivariate correlations analyzed between steady-post-BCVA and all MH parameters

Parameters	*r*	*P*
Age	0.175	0.205
Duration time	-0.152	0.272
Height	-0.069	0.619
DHI	0.058	0.680
VRF	0.072	0.605
BD	0.521	<0.001
MD	0.514	<0.001
MHI	-0.531	<0.001
THI	-0.386	0.004
HFF	-0.508	<0.001
ARF	-0.532	<0.001

Bivariate correlations were analyzed between logMAR steady-post-BCVA and all MH parameters by the Pearson method. Table 1 shows the r and P values. The characteristic parameters such as age (r=0.175, P=0.205), duration (r= -0.152, P=0.272), height (r=-0.069, P=0.619), DHI (r=0.058, P=0.680), and VRF (r=0.072, P=0.605) were not statistically significant. Others including BD (r=0.521, P<0.001), MD (r=0.514, P<0.001), MHI (r=-0.531, P<0.001), THI (r=-0.386, P=0.004), HFF (r=-0.508, P<0.001), and ARF (r=-0.532, P<0.001) were statistically significant.

ROC curves analyses were performed to further discuss the different parameters on the prediction of visual outcome. Positive correlation parameters are presented in Figure 4A. Other negative correlation parameters are displayed in Figure 4B.

Table 2 details the AUC, cut-off value, and associated sensitivity and specificity with MD, BD, MHI, THI, HFF, and ARF. According to AUC values, values of ARF, MHI, HFF, MD, THI, and BD are 0.806, 0.772, 0.750, 0.705, 0.690, and 0.686 respectively. The associated cut-off value, sensitivity, and specificity, respectively, are as follows: ARF (1.558, 0.769, and 0.786); MHI (0.427, 0.885, and 0.607); HFF (1.027, 0.731, and 0.714); MD (416, 0.679, and 0.654); THI (1.710, 0.577, and 0.821); and BD (868, 0.714, and 0.647).

Table 2 AUC, cut-off value, associated sensitivity and specificity with min diameter, BD, MHI, THI, HFF and ARF

Parameters	AUC	P	Cut-off point		
			Value	Sensitivity	Specificity
MD	0.705	0.010	416	0.679	0.654
BD	0.686	0.019	868	0.714	0.647
MHI	0.772	0.001	0.427	0.885	0.607
THI	0.690	0.017	1.710	0.577	0.821
HFF	0.750	0.002	1.027	0.731	0.714
ARF	0.806	<0.001	1.558	0.769	0.786

DISCUSSION

This paper proposed the parameter ARF, which could effectively predict postoperative visual acuity. High ARF value represents that MH peripheral tissues might be effective to fill the macular concave center area, which indicates better visual recover y after surgery. Similar to MHI, HFF, MD, THI, and BD steady-post-BCVA analyzed with bivariate correlations for ARF was found statistically significant. Furthermore, ROC curves analysis for above six parameters was performed to further discuss the different parameters on the prediction of steady-post-BCVA. ROC curve analysis found that the proposed ARF had best prediction power.

This study has the following limitations. First, although the number of samples might be more than that reported in some studies, the overall sample size is relatively small. Second, we utilized the clinical case series of Affiliated Hospital of Nantong University Eye Center. Third, manual segmentation, single slice, and the specific model of the OCT machine, might have resulted in discrepant findings across studies that used the same method. As we used the Meshlab to generate the 3D MH and measure specific regions and parameters with built-in functions of the software, this process may have introduced some deviation. Due to the limitations of our sample, we didn't find a correlation between the steady-post-BCVA and the duration of symptoms in this study. While, it is a clinical experience and result of various studies[22-25] that a longer duration of 6 or 12mo negative influences the vision rehabilitation after surgery.

In future studies, we plan to gather more data samples and design effective automated segmentation, 3D reconstruction, and measurement algorithms, wherein automatic algorithms are used instead of manual operations to reduce the deviation and improve the accuracy of the experiment. There are few public OCT images network dataset, which contain very small number of samples or very low image resolution. The OCT database of MH samples, including GETOCT[26], retinal OCT imaging[27] and New York Eye Ear Infirmary of Mount Sinai (NYEE), were found on the internet. While GETOCT only released several medical records, retinal OCT imaging did not focus on our research theme, and NYEE images were of very low image resolution and thereby unclear. Therefore, we utilized the clinical case series of Nantong University Affiliated Hospital Eye Center.

In conclusion, based solely on the MH's unique 3D morphological characteristics, this study has designed, built, and verified the 3D index type ARF for postoperative analysis of the MH. Medical statistical analysis results indicate that the ARF, compared with traditional 2D index, provide more effective sensitivity and specificity.

ACKNOWLEDGEMENTS

Foundations: Supported by National Natural Science Foundation of China (No.61675124; No.81501559); Natural Science Foundation of the Higher Education Institutions of Jiangsu Province, China (No.15KJB310015); Science and Technology Foundation of Nantong Technology Bureau (No. MS12015180).

Conflicts of Interest: Geng XY, None; **Wu HQ,** None; **Jiang JH,** None; **Jiang K,** None; **Zhu J,** None; **Xu Y,** None; **Dong JC,** None; **Yan ZZ,** None.

REFERENCES

1 Ruiz-Moreno JM, Staicu C, Piñero DP, Montero J, Lugo F, Amat P. Optical coherence tomography predictive factors for macular hole surgery outcome. *Br J Ophthalmol* 2008;92(5):640-644.

2 Puliafito CA, Hee MR, Lin CP, Reichel E, Schuman JS, Duker JS, Izatt JA, Swanson EA, Fujimoto JG. Imaging of macular diseases with optical coherence tomography. *Ophthalmology* 1995;102(2):217-229.

3 Nukada K, Hangai M, Ooto S, Yoshikawa M, Yoshimura N. Tomographic features of macula after successful macular hole surgery. *Invest Ophthalmol Vis Sci* 2013;54(4):2417-2428.

4 Kusuhara S, Negi A. Predicting visual outcome following surgery for idiopathic macular holes. *Ophthalmologica* 2014;231(3):125-132.

5 Chen H, Chen W, Zheng K, Peng K, Xia H, Zhu L. Prediction of spontaneous closure of traumatic macular hole with spectral domain optical coherence tomography. *Sci Rep* 2015;5:12343.

6 Matsumiya W, Kusuhara S, Shimoyama T, Honda S, Tsukahara Y, Negi A. Predictive value of preoperative optical coherence tomography for visual outcome following macular hole surgery: effects of imaging alignment. *Jpn J Ophthalmol* 2013;57(3):308-315.

7 Ullrich S, Haritoglou C, Gass C, Schaumberger M, Ulbig MW, Kampik A. Macular hole size as a prognostic factor in macular hole surgery. *Br J Ophthalmol* 2002;86(4):390-393.

8 Kusuhara S, Teraoka Escaño MF, Fujii S, Nakanishi Y, Tamura Y, Nagai A, Yamamoto H, Tsukahara Y, Negi A. Prediction of postoperative visual outcome based on hole configuration by optical coherence tomography in eyes with idiopathic macular holes. *Am J Ophthalmol* 2004;138(5):709-716.

9 CIRRUS HD-OCT. http://www.zeiss.com.cn/meditec/products/ophthalmology-optometry/glaucoma/diagnostics/optical-coherence-thomography/cirrus-family/cirrus-hd-oct.html (Accessed on Oct 22, 2016).

10 3D OCT-1 Maestro, Optical Coherence Tomographer. http://www.topcon-medical.eu/eu/products/253-3d-oct-1-maestro-optical-coherence-tomography.html#description (Accessed on Oct 20, 2016).

11 Introducing the SPECTRALIS glaucoma module premium edition. https://business-lounge.heidelbergengineering.com/us/news/news/introducing-the-spectralis-glaucoma-module-premium-edition-98365007 (Accessed on Oct 26, 2016).

12 Scheibe P, Lazareva A, Braumann UD, Reichenbach A, Wiedemann P, Francke M, Rauscher FG. Parametric model for the 3D reconstruction of individual fovea shape from OCT data. *Exp Eye Res* 2014;119(1):19-26.

13 Haas P, Esmaeelpour M, Ansari-Shahrezaei S, Drexler W, Binder S. Choroidal thickness in patients with reticular pseudodrusen using 3D 1060-nm OCT maps. *Invest Ophthalmol Vis Sci* 2014;55(4):2674-2681.

14 Brionesr MDJ, Torreibarra MHDL, Santoyo FM. 3D optical phase reconstruction within PMMA samples using a spectral OCT system. *Proc SPIE* 2015;9660:318-324.

15 Todorich B, Shieh C, DeSouza PJ, Carrasco-Zevallos OM, Cunefare DL, Stinnett SS, Izatt JA, Farsiu S, Mruthyunjaya P, Kuo AN, Toth CA. Impact of microscope-integrated OCT on ophthalmology resident performance of anterior segment surgical maneuvers in model eyes. *Invest Ophthalmol Vis Sci* 2016;57(9):OCT146-153.

16 Hu Z, Girkin CA, Hariri A, Sadda SR. Three-dimensional choroidal segmentation in spectral OCT volumes using optic disc prior information. *Proc SPIE* 2016;9697:57-63.

17 Steel DH, Parkes C, Papastavrou VT, Avery PJ, EI-Ghrably IA, Habib MS, Sandinha MT, Smith J, Stannard KP, Vaideanu-Collins D, Hillier RJ. Predicting macular hole closure with ocriplasmin based on spectral domain optical coherence tomography. *Eye (Lond)* 2016;30(5):740-745.

18 Grewal DS, Fine HF, Mahmoud TH. Management of challenging macular holes: current concepts and new surgical techniques. *Ophthalmic Surg Lasers Imaging Retina* 2016;47(6):508-513.

19 Shpak AA, Shkvorchenko DO, Sharafetdinov IKh, Yukhanova OA. Predicting anatomical results of surgical treatment of idiopathic macular hole. *Int J Ophthalmol* 2016;9(2):253-257.

20 Parravano M, Giansanti F, Eandi CM, Yap YC, Rizzo S, Virgili G. Vitrectomy for idiopathic macular hole. *Cochrane Database Syst Rev* 2015;5:CD009080.

21 Holladay JT. Proper method for calculating average visual acuity. *J Refract Surg* 1997;13(4):388-391.

22 Mitchell P, Korobelnik JF, Lanzetta P, Holz FG, Prünte C, Schmidt-Erfurth U, Tano Y, Wolf S. Ranibizumab (Lucentis) in neovascular age-related macular degeneration: evidence from clinical trials. *Br J Ophthalmol* 2010;94(1):2-13.

23 Keane PA, Patel PJ, Liakopoulos S, Heussen FM, Sadda SR, Tufail A. Evaluation of age-related macular degeneration with optical coherence tomography. *Surv Ophthalmol* 2012;57(5):389-414.

24 Inoue M, Arakawa A, Yamane S, Watanabe Y, Kadonosono K. Long-term outcome of macular microstructure assessed by optical coherence tomography in eyes with spontaneous resolution of macular hole. *Am J Ophthalmol* 2012;153(4):687-691.

25 Sharma D, Venkatesh R, Mayor R, Agarwal M. Spectral-domain optical coherence tomography study of macular structure as prognostic and determining factor for macular hole surgery outcome. *Retina* 2014;34(3):e5.

26 *Free cases impressions from GETOCT*. http://www.getoct.ch/index.php?site=cases (Accessed on Oct 26, 2016).

27 *Retinal OCT imaging*. http://www.opsweb.org/?page=RetinalOCT (Accessed on Oct 26, 2016).